Effects of pH value and Sintering Temperature on the Structural and Magnetic Properties of Barium Hexaferrites Prepared by Co-Precipitation

EMAN S. AL-HWAITAT[1], MOHAMMAD K. DMOUR[1], AHMAD S. MASADEH[1], YAZAN MASWADEH[2], IBRAHIM BSOUL[3] and SAMI H. MAHMOOD[1,4]*

[1]Physics Department, The University of Jordan, Amman 11942, Jordan.
[2]Department of Physics, Central Michigan University, Mt. Pleasant, MI 48859, USA.
[3]Physics Department, Al al-Bayt University, Mafraq 13040, Jordan.
[4]Department of Physics and Astronomy, Michigan State University, East Lansing, MI 48824, USA.

Abstract

Barium hexaferrite ($BaFe_{12}O_{19}$; M-type; BaM) is an important, cost effective magnetic material for permanent magnet applications. The magnetic properties of the prepared samples, and the purity of the BaM phase depend critically on the synthesis route and experimental conditions. In this study, BaM hexaferrites were prepared by co-precipitation method using two different values of pH for the precursor solutions (11.0 and 12.5), and sintering pellets of the co-precipitates at 860, 920 and 990°C. The prepared samples were characterized using X-ray diffraction and magnetic measurements. X-ray diffraction patterns indicated that the samples prepared with pH = 12.5 consisted of a single BaM phase at all sintering temperatures. However, the patterns of the samples with pH = 11.0 did not reveal the existence of BaM at 860°C, whereas a major BaM phase (86 – 87 wt.%) was observed at 920 and 990°C with a minor α-Fe_2O_3 phase. The thermo magnetic curves confirmed the BaM magnetic phase in the samples. The hysteresis loops of the BaM samples showed characteristics of hard magnetic materials with relatively high saturation magnetization. Analysis of the magnetic data indicated an intrinsic coercivity $H_{ci} \sim 5$ kOe for all samples, and a saturation specific magnetization in the range $\sigma_s = 56.0 – 66.3$ emu/g, which are suitable for permanent magnet applications. The practical coercivity (H_{cB}), residual induction (B_r) and maximum energy product $(BH)_{max}$ of the samples with pH = 12.5 are higher than those of the samples with pH = 11.0, and the highest magnetic parameters of H_{cB} = 1871 Oe, B_r = 2384 G, and $(BH)_{max}$ = 8.92 kJ/m³ were observed for the sample with pH = 12.5 and sintered at 860°C.

CONTACT Sami H.Mahmood ✉ s.mahmood@ju.edu.jo 📍 Department of Physics and Astronomy, Michigan State University,East Lansing, MI 48824, USA.

Introduction

M-type hexaferrite of chemical formula $AFe_{12}O_{19}$ (A = Ba, Sr, Pb) belongs to an important class of magnetic oxides exhibiting a wide range of interesting industrial and technological applications, including permanent magnet, magnetic recording, microwave absorption and microwave devices.[1-10] This range of applications can be facilitated by controlled tuning of the properties of BaM, which can be achieved by special substitutions for A^{2+} and /or Fe^{3+} ions, and by modifying the synthesis route as described by recent review articles.[11-13] The improvement of the characteristics of a material for permanent magnet applications involves the simultaneous increase of its coercivity and remnant magnetization. On the other hand, tailoring the properties of the material for magnetic recording involves the control of the coercivity in the range of 1 – 3 kOe, while maintaining a high remnant magnetization (typically above 20 emu/g).

The method of preparation, the adopted experimental conditions including stoichiometry and sintering temperature, and controlling the particle size distribution of the ceramic powder play important role in determining the magnetic properties of BaM. Recently, the effects of synthesis method (ball milling versus sol-gel method), cationic substitutions, and sintering temperature on the magnetic properties of M-type hexaferrites for permanent magnet applications demonstrated high sensitivity to these experimental parameters.[14, 15] While low sintering temperatures (< 1000°C) are required for preparing M-type hexaferrites with single domain magnetic particles and enhanced coercivity, it is difficult to prepare a high purity phase by conventional ceramic method or ball milling using such low sintering temperatures, which leads to lower magnetic parameters. Alternatively, researchers have used special substitution scenarios to produce M-type hexaferrites with high coercivities suitable for high quality permanent magnets.[15-21] However, in several cases, the improvement of the coercivity was accompanied by some drawbacks such as unfavorable decrease of the saturation and remnant magnetizations, the use of expensive rare-earth elements, and elaborate experimental procedures.[20-24]

Co-precipitation technique was reported to be successful for the preparation of M-type hexaferrites with controlled particle size distribution and enhanced coercivity at low sintering temperatures.[25-27] The effects of stoichiometry, heat treatment, and pH on the formation of the hexaferrite phase and its magnetic properties were addressed by several researchers.[28-31] The reported results indicated large variations of the magnetic properties, and sensitivity to the details of the experimental procedures. The observed deterioration of certain magnetic parameters such as the saturation magnetization could be associated with nonmagnetic impurity phases coexisting with the M-type hexaferrite phase, whereas the deterioration of the coercivity could be associated with particle morphology and particle-size distribution. This study is concerned with optimizing the experimental conditions for the production of high-quality BaM ($BaFe_{12}O_{19}$) hexaferrites by coprecipitation of stoichiometric solutions of iron and barium nitrates. The effects of pH and heat treatment on the phase purity of BaM, and its structural and magnetic properties are investigated.

Experimental Techniques

Co-precipitation method was adopted for the preparation of BaM hexaferrites using high-purity (≥ 99%) $Ba(NO_3)_2$ and $Fe(NO_3)_3.9H_2O$ starting powders. Stoichiometric amounts of the starting powders were used to prepare the starting solutions by dissolving the metal nitrates in distilled water. The solutions were mixed, and the ferrite precursor was precipitated from this mixture by adding 6M NaOH solution drop wise with the pH of the solution adjusted to 11.0 or 12.5. The solution containing the precipitate was centrifuged at 7000rpm for 2 min., and the powder precipitate was separated and washed with D.I. water ten times. The powder was then dried at 100°C for (4-8) hrs. Disk-shaped pellets were prepared using a hydraulic press and a force of 50 kN, and sintered in air at 860, 920 and 990°C for 2 h.The synthesized samples were characterized using X-ray diffraction (XRD), and vibrating sample magnetometry (VSM).

Results and Discussion
XRD Results

Fig. 1 shows XRD patterns for all samples prepared at pH = 11.0 and 12.5, and sintered at different temperatures. The pattern of the sample with pH = 11.0 and sintered at 860ºC indicated the presence of a major α-Fe_2O_3 oxide phase (JCPDS: 01-079-1741), and other unidentified peaks (labelled by β)

indicated the presence of a secondary Ba-containing minor phases. However, XRD patterns for the samples with pH = 11.0 and sintered at 920°C and 990°C revealed the evolution of a major BaM hexaferrite phase (JCPDS: 00-043-0002), in addition to a small amount of α-Fe_2O_3 phase represented by the weak peaks corresponding to its structural reflections.On the other hand, XRD patterns of the samples prepared at pH = 12.5 indicated the presence of a single BaM phase at all sintering temperatures, without any additional secondary phases. By comparing the patterns of the samples prepared at pH = 11.0, we notice the sensitivity of the formation of BaM phase to the sintering temperature. However, with pH = 12.5, the formation temperature of a pure BaM phase was significantly

lowered, where a pure BaM phase was observed at 860°C without any secondary phase, indicating the sensitivity of the purity of BaM phase to the pH value. In comparison, the coexistence of a secondary phase with the major BaM phase in samples sintered at 920°C, and with pH = 12.0 and 12.5, was reported in a previous study.[25] The higher quality of our samples in terms of phase purity could be attributed to adopting different experimental conditions such as the starting materials (iron and barium nitrates rather than iron and barium chlorides), and Fe/Ba ratio (12 rather than 10 – 11). These results indicate that all experimental conditions, starting materials, pH value, heat treatment, and chemical stoichiometry, need to be optimized for the production of high quality M-type hexaferrites.
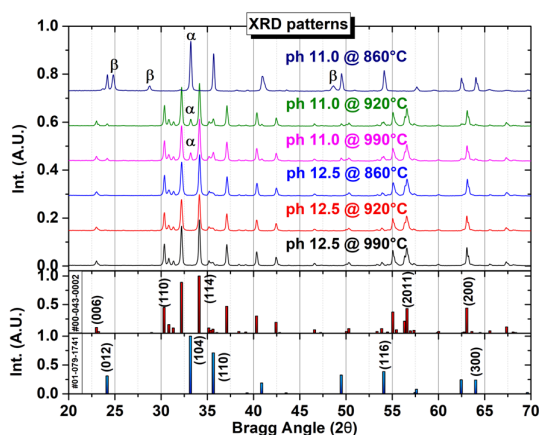

Fig. 1: XRD patterns for the samples prepared with the indicated pH value and sintering temperature. The peaks in the top pattern correspond to α-Fe_2O_3 phase (α), whereas those corresponding to the unidentified phase are labelled by (β).The JCPDS standard patterns of BaM (00-043-0002) and α-Fe_2O_3 (01-079-1741) are included for comparison
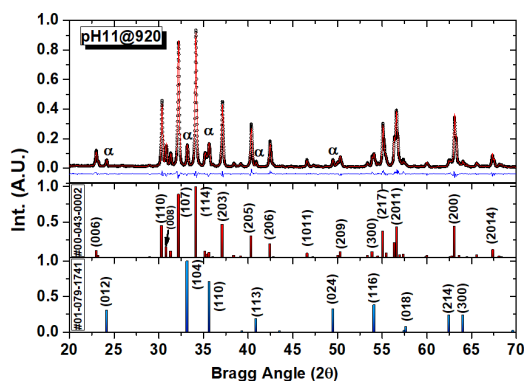

Fig. 2: XRD pattern with Rietveld refinement for the samplewith pH = 11.0 and sintered at 920°C. The blue line under the pattern represents the difference between the experimental data and theoretical fit. The standard patterns for BaM and α-Fe_2O_3 phase are shown for comparison

To determine the refined structural parameters and the weight percent (wt.%) of the phases in the samples, the XRD patterns were refined by Rietveld analysis using Full Prof software. Fig. 2 shows a representative Rietveld-refined XRD pattern for the sample with pH = 11.0 sintered at 920°C. The refined atomic parameters used to simulate the experimental pattern are shown in Table 1. The quality of fit for all patterns was very good as indicated by comparing the experimental data (black circles) with the theoretical pattern (red line), and by the horizontal difference curve (blue line representing the difference between the experimental data and the theoretical fit). The high quality of the fit was also indicated by the low values of the reliability factors (Bragg (R_B) and structure factor (R_F) reliability factors in Table 2).Table 2 shows the refined lattice parameters (a and c), cell volume (V), and X-ray density (ρ_x), whereas Table 3 shows the wt.% of phases in the samples containing BaM phase.

The refined lattice parameters a = (5.8889 ±0.0032) Å and c = (23.199± 0.010) Å of the BaM phase in all samples are in good agreement with the reported values for BaM hexaferrites[32, 33]. Also, the refined X-ray density of ρ_x = (5.299 ± 0.007) g/cm is in good agreement with reported values for BaM samples. The results also indicated that the samples with pH = 11.0 and sintered at 920°C and 990°C consisted of a major BaM phase (87 wt.% and 86 wt.%, respectively), in addition to a secondary α-Fe_2O_3 phase (13 wt.% and 14 wt.%, respectively), whereas the samples with pH = 12.5 consisted of a pure BaM phase at all sintering temperatures. These results confirm our qualitative discussion of the XRD patterns in the first paragraph of this section.

Table 1: The refined atomic parameters of the BaM phase used to simulate the experimental pattern in Fig. 2

Atom	Site	Symmetry	x/a	y/b	z/c
Ba	2d	-6m2	2/3	1/3	1/4
Fe1	2a	-3m.	0	0	0
Fe2	2b	-6m2	0	0	1/4
Fe3	4f	3m.	1/3	2/3	0.02755
Fe4	4f	3m.	1/3	2/3	0.19052
Fe5	12k	.m.	1/6	1/3	0.89151
O1	4e	3m.	0	0	0.15427
O2	4f	3m.	1/3	2/3	0.9467
O3	6h	mm2	1/6	1/3	1/4
O4	12k	.m.	1/6	1/3	0.0518
O5	12k	.m.	1/2	1	0.14956

Table 2: BaM lattice constant and cell volume, X-ray density, and reliability factors

Sample	a (Å)	c (Å)	V (Å³)	ρ_x (g/cm³)	R_B	R_F
pH11@920	5.8885	23.200	696.69	5.298	2.82	2.33
pH11@990	5.8890	23.202	696.86	5.297	2.64	2.23
pH12.5@860	5.8857	23.189	695.68	5.306	3.38	2.66
pH12.5@920	5.8913	23.205	697.50	5.292	2.94	2.62
pH12.5@990	5.8901	23.201	697.07	5.296	2.32	1.98

Table 3: Weigh ratios of BaM and α-Fe_2O_3 phases determined by the refinement of the XRD data of each sample

pH	11.0		12.5		
T (°C)	920	990	860	920	990
BaM wt.%	87	86	100	100	100
α-Fe_2O3 wt.%	13	14	0	0	0

Magnetic Measurements
Isothermal Magnetization
The magnetic properties of the samples were measured by VSM at room temperature in a magnetic field up to 10 kOe. The hysteresis loops of all samples are shown in Fig. 3. The hysteresis loop of the sample with pH = 11.0 sintered at 860°C exhibited almost a linear behaviour, with a weak magnetization (~ 1 emu/g at the maximum field of 10 kOe), and a small opening in the central region. This result is consistent with the structural analysis, where the magnetic behaviour is attributed to the weakly ferromagnetic behaviour of α-Fe_2O_3exhibiting canted antiferromagnetic structure at room temperature.[34] This canted spin structure is maintained from Morin Temperature (~ 260 K)up to Neel temperature (~ 955 K).[35] Similar behaviour with maximum magnetization of 0.31 – 1.30 emu/g was observed in commercial α-Fe_2O_3 powders.[36] However, the hysteresis loops of all other samples are wide, and demonstrated tendency toward saturation at high fields, which is characteristic of the behaviour of hard magnetic materials. These results are also consistent with the XRD results which revealed the presence of a major BaM phase in these samples.
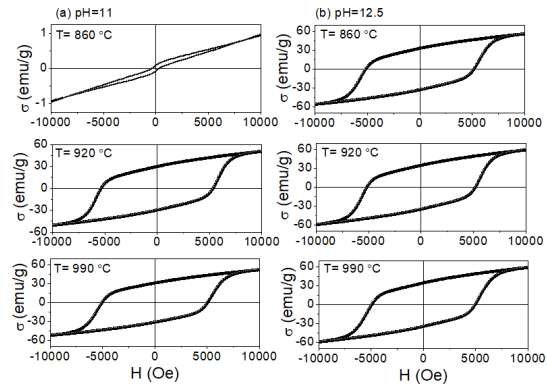

Fig. 3: Hysteresis loops of the samples prepared by co- precipitation with (a) pH = 11.0,(b) pH = 12.5, and sintered at different temperatures

Table 4: Saturation magnetization (σ_s), remanence(σ_r), squareness ratio ($\sigma_{rs} = \sigma_r/\sigma_s$), intrinsic coercivity (H_{ci}), magnetic anisotropy field (H_a), and first anisotropy constant (K_1)for the samples containing a major BaM phase

pH	Sintering Temperature	σ_s(emu/g)	σ_r (emu/g)	σ_{rs}	H_{ci}(kOe)	H_a (kOe)	K_1 (10^6erg/cm^3)
11.0	920°C	56.0	29.8	0.53	5.33	12.4	1.84
	990°C	58.0	31.2	0.54	5.03	12.4	1.91
12.5	860°C	58.6	33.1	0.56	5.14	13.0	2.02
	920°C	66.3	35.0	0.53	5.17	12.6	2.21
	990°C	65.9	34.7	0.53	4.93	12.4	2.16

The saturation specific magnetization (σ_s) of each sample was obtained from the Law of Approach to Saturation in the high-field range.[34] In the field range H = 8.5 – 10 kOe, the specific magnetization (σ) was found to obey the relation $\sigma= \sigma_s(1 – B/H^2)$, where B is a constant representing the magnetocrystalline anisotropy, indicating that the magnetization behaviour can be described by the magnetocrystalline anisotropy contribution.[37] The values of σ_s obtained from the linear fit to the σ vs. $1/H^2$ plots (not shown for brevity), as well as the remnant specific magnetization (σ_r) and the intrinsic coercivity (H_{ci}) obtained from the hysteresis loops are listed in Table 4. In addition, the values of the magnetocrystalline anisotropy field (H_a), and the first anisotropy constant (K_1) were determined from the constant B using the relation[38]

$$B = \frac{H_a^2}{15} = \frac{1}{15}\left(\frac{2K_1}{\sigma_s}\right)^2 \qquad ...(1)$$

The values of these magnetic parameters are also listed in Table 4.

The values of σ_s and σ_r for the samples prepared with pH = 12.5 are significantly higher than those of the samples prepared with pH = 11.0 at all sintering temperatures. The improvement of σ_s for the samples prepared with pH = 12.5 is attributed to the higher purity of the BaM phase in these samples as demonstrated by their XRD patterns. The maximum

value of σ_s= 66.3 emu/g and σ_r= 35.0 emu/g for the sample with pH =12.5 and sintered at 920°C are somewhat higher than σ_s = 62.2 emu/g and σ_r = 33.6 emu/grecently reported for BaM sample prepared by ball milling and sintered at 1100°C.[14] Also, the highest saturation magnetization obtained by our group is close to the maximum value of 68 emu/g recently reported for BaM sample prepared by coprecipitation with pH = 13 and sintered at1000°C.[39] However, the observed intrinsic coercivity of H_{ci} = 5.13 ± 0.20 kOe for all samples in this study is significantly higher than 2.67 – 3.61 kOe or 2.40 – 4.40 kOe reported in the two above mentioned studies, respectively. Considering that the coercivity is an important parameter of hard magnetic materials, the results demonstrate that our method provided a high purity BaM hexaferrite at relatively low sintering temperatures for permanent magnet applications. Low sintering temperatures are important to obtain single domain particles by avoiding particle growth at higher sintering temperatures. The single domain nature of the prepared samples is evidenced by squareness

ratio σ_{rs} (Table 4), being slightly higher than the value of ~ 0.5 characteristics of an assembly of randomly oriented, single-domain magnetic particles (multi-domain particles exhibit a squareness ratio < 0.5).

The magnetocrystalline anisotropy field for the samples fluctuated by ~ 2% around the average value (H_a = 12.7± 0.3 kOe), whereas the first anisotropy constant K_1increased at pH = 12.5 by about 20% (from 1.84×10^6 to 2.21×10^6 erg/cm^3) at sintering temperature 920°C, and by about 13% (from 1.91×10^6 to 2.16×10^6 erg/cm^3) at sintering temperature 990°C. The lower values of K_1 for the samples prepared at pH = 11.0 do not necessarily indicate a reduction of the magnetocrystalline anisotropy of the BaM phase in these samples, but rather, could be attributed to the lower saturation magnetization due to the impurity phases. The observed values of the anisotropy field and first anisotropy constant are in good agreement with values reported for BaM prepared by ball milling and sol-gel methods.[14]
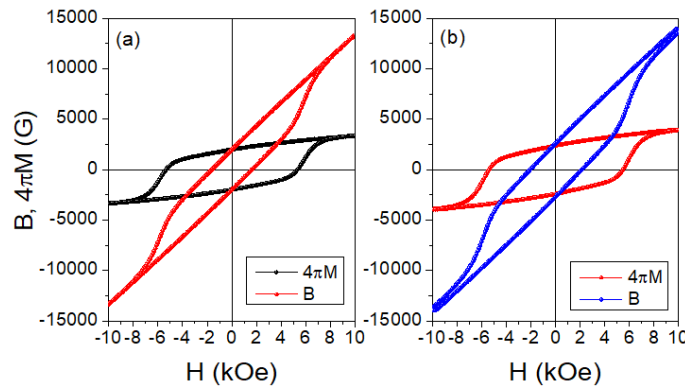

Fig. 4: Representative hysteresis loops of the magnetic induction (B) and (4πM) for the two samples sintered at 920 °C:(a) the sample with pH =11.0and (b) the sample with pH =12.5.

Further analysis of the magnetization data involves determination of the maximum energy product, and investigating the linearity of the B-H curve in the second quadrant (demagnetization curve) of the hysteresis loop. These are two key quality parameters for permanent magnet applications.[40] The magnetic induction B = H + 4πM, where the magnetization(M) is the product of the specific magnetization (σ) and the density(M = ρ×σ). Fig. 4 shows representative hysteresis loops of B and 4πM for the samples sintered at 920°C. The portion

of the B-H curve in the second quadrant is shown in Fig. 5 for all samples. The linear behaviour indicates stability of these materials against stray fields in motor operation at relatively high temperatures.[41] The practical coercivity H_{cB} (also called the coercivity H_c),as well as the residual induction (B_r), were determined from these curves, and the results are listed in Table 5. The data revealed higher magnetic properties of the samples prepared with pH = 12.5 compared to the samples prepared with pH = 11.0. Also, the ranges of coercivity (H_{cB} = 1825 –

1871 Oe) and B_r = 2308 –2384 G for the samples prepared with pH = 12.5 indicated improvement of the magnetic properties compared to BaM samples prepared by sol-gel method and sintered at similar temperatures.[14]

Table 5: Magnetic parameters for the samples prepared byco- precipitation method

pH	Sintering Temperature	B_r (G)	H_{cB}(Oe)	$(BH)_{max}$ (kJ/m³)
11.0	920 °C	1982	1628	6.45
	990 °C	2075	1709	6.85
12.5	860 °C	2384	1871	8.92
	920 °C	2323	1844	8.52
	990 °C	2308	1825	8.36
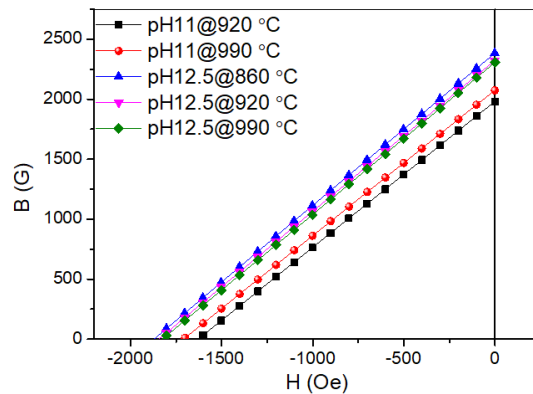
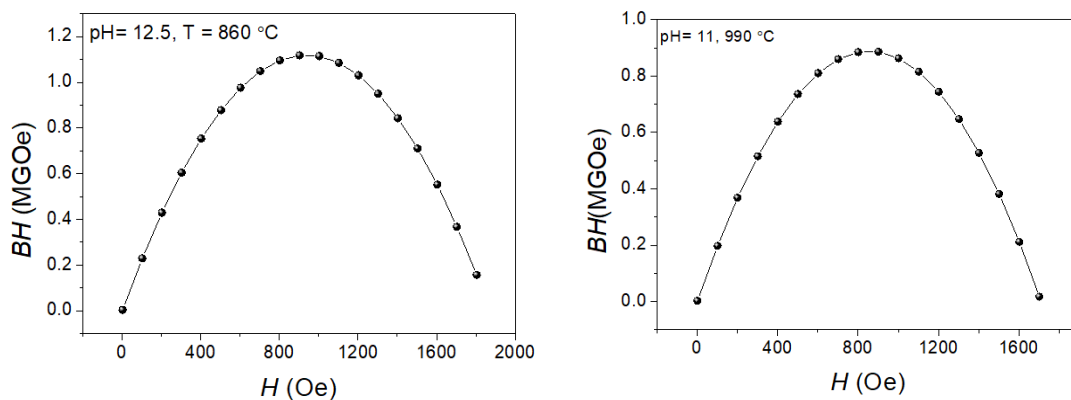**Fig. 5: B-H curves in the second quadrant of the hysteresis loop for all samples**

Fig. 6: BH vs. *Hcurves* in the second quadrant of the hysteresis loop for the samples with pH12.5 @860, and pH11@990. 1 MGOe = 7.96 kJ/m³

An important figure of merit for a permanent magnetic material is the maximum energy product $(BH)_{max}$, which can be determined from the plots BH vs. H in the second quadrant of the hysteresis loop (representative curves are shown in Fig. 6). The maximum energy product (1 MGOe = 7.96 kJ/m³) for all samples are shown in Table 5. The results indicated that the sample with pH =

12.5 exhibited higher maximum energy products than the samples with pH = 11.0. The data in Table 5 indicated that the sample with pH = 12.5 sintered at 860 exhibited the highest magnetic parameters. Although these parameters are not competitive with rare-earth magnets' parameters,[41] the alignment of the particles (by a magnetic field) can double the residual induction (considering the squareness ratio of ~ 0.5), and increase the maximum energy product by a factor of four, thus providing cost-effective magnetic materials.

Thermomagnetic Measurements

A powerful complementary tool for materials characterization is the measurement of the magnetization versus temperature at a constant weak applied magnetic field, to determine the magnetic phases in the sample from their respective magnetic phase transition temperatures. Fig. 7 shows the magnetization vs. temperature curves for the samples under an applied magnetic field of 100 Oe. The thermomagnetic curves revealed a single phase transition (characterized by the Curie temperature indicated by the arrows in Fig. 7) in all samples, indicating the presence of one magnetic phase. Notice that the α-Fe_2O_3 phase in the samples with pH = 11.0 does not exhibit magnetic phase transition in the range of temperature adopted in the study (as mentioned above). The Hopkinson peak just below the Curie temperature indicates the presence of small, super paramagnetic particles in the samples.[42] The Curie temperature of $(450 \pm 10)°C$ for the samples is in agreement with ferromagnetic-to-paramagnetic transition temperature of the BaM phase (450 °C).[32]
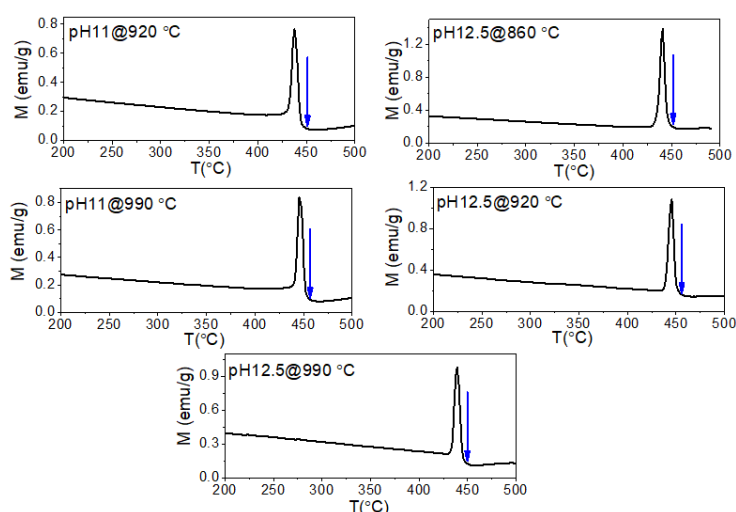

Fig. 7: Thermomagnetic curves (at an applied field of 100 Oe) for the samples

Conclusions

The phase formation temperature and the purity of BaM hexaferrite in samples prepared by co-precipitation of metal and barium nitrates demonstrated sensitivity to the pH value of the stoichiometric precursor solution. All samples prepared with pH =12.5 and sintered at temperatures from 860°C to 990°C revealeda single BaM hexaferrite phase with no secondary phases, whereas the samples with pH = 11.0 revealed the presence of a major BaM phase at sintering temperatures of 920°C to 990°C, with a minor α-Fe_2O_3 phase. The magnetic parameters of the samples with pH = 12.5 were higher than those with pH = 11.0. The results of the study indicated that improvement of the magnetic properties of BaM hexaferrite can be achieved by adopting a suitable synthesis route, and tuning the experimental conditions. The samples prepared with pH = 12.5 demonstrated improved magnetic properties suitable for permanent magnet applications. Based on the results of this study, we anticipate that the preparation of anisotropic magnets with a high degree of alignment of the easy axis of the particles prepared by this method could give magnets with high residual induction of ~ 4760 G, and maximum

energy product of ~ 35 kJ/m³. These parameters are close to the theoretical values of B_r ~ 4780 G and $(BH)_{max}$ ~ 45 kJ/m³.

Conflict of interest

The author declares that they have no conflict of interest.

References

1. R.C. Pullar, Hexagonal ferrites: a review of the synthesis, properties and applications of hexaferrite ceramics, *Progress in Materials Science*, 57 (2012) 1191-1334.

2. V.G. Harris, A. Geiler, Y. Chen, S.D. Yoon, M. Wu, A. Yang, Z. Chen, P. He, P.V. Parimi, X. Zuo, Recent advances in processing and applications of microwave ferrites, *Journal of Magnetism and Magnetic Materials,* 321 (2009) 2035-2047.

3. V.G. Harris, Z. Chen, Y. Chen, S. Yoon, T. Sakai, A. Gieler, A. Yang, Y. He, K. Ziemer, N.X. Sun, Ba-hexaferrite films for next generation microwave devices, *Journal of Applied Physics*, 99 (2006) 08M911.

4. S.H. Mahmood, Permanent Magnet Applications, in: S.H. Mahmood, I. Abu-Aljarayesh (Eds.) Hexaferrite Permanent Magnetic Materials, *Materials Research Forum LLC, Millersville,* PA, 2016, pp. 153-165.

5. U. Topal, H.I. Bakan, Permanently magnetic BaFe12O19 foams: Synthesis and characterization, *Materials Chemistry and Physics,* 123 (2010) 121-124.

6. J. Nicolas, Microwave ferrites, in: E.P. Wohlfarth (Ed.) Ferromagnetic Materials, North-Holland Publishing Company, New York, 1980, pp. 243-296.

7. G. Bate, Magnetic recording materials since 1975, *Journal of Magnetism and Magnetic materials,* 100 (1991) 413-424.

8. M.N. Ashiq, M.J. Iqbal, M. Najam-ul-Haq, P.H. Gomez, A.M. Qureshi, Synthesis, magnetic and dielectric properties of Er–Ni doped Sr-hexaferrite nanomaterials for applications in High density recording media and microwave devices, *Journal of Magnetism and Magnetic Materials*, 324 (2012) 15-19.

9. S.H. Mahmood, A.M. Awadallah, Y. Maswadeh, I. Bsoul, Structural and magnetic properties of Cu-V substituted M-type barium hexaferrites, IOP Conference Series: *Materials Science and Engineering*, 92 (2015) 012008.

10. S.H. Mahmood, A.A. Ghanem, I. Bsoul, A. Awadallah, Y. Maswadeh, Structural and magnetic properties of $BaFe_{12-2x}Cu_xMn_xO_{19}$ hexaferrites, *Materials Research Express*, 4 (2017) 036105.

11. S.H. Mahmood, I. Bsoul, Tuning the magnetic properties of M-type hexaferrites, in: R.B. Jotania, S.H. Mahmood (Eds.) Magnetic Oxides and Composites, *Materials Research Forum LLC, Millersville,* PA, USA, 2018, pp. 49-100.

12. S.H. Mahmood, Properties and Synthesis of Hexaferrites, in: S.H. Mahmood, I. Abu-Aljarayesh (Eds.) Hexaferrite Permanent Magnetic Materials, *Materials Research Forum LLC, Millersville*, PA, 2016, pp. 74-110.

13. S.H. Mahmood, Ferrites with High Magnetic Parameters, in: S.H. Mahmood, I. Abu-Aljarayesh (Eds.) Hexaferrite Permanent Magnetic Materials, *Materials Research* Forum LLC, Millersville, PA, 2016, pp. 111-152.

14. E.S. Al-Hwaitat, M.K. Dmour, I. Bsoul, R. Al-Buqain, S.H. Mahmood, A comparative study of $Ba_xSr_{1-x}Fe_{12}O_{19}$ ferrite permanent magnets prepared by ball milling and sol–gel routes, *Journal of Physics D: Applied Physics, (*2020).

15. Ghada A. Al-Garalleh, I. Bsoul, Y. Maswadeh, Eman S. Al-Hwaitat, Sami H. Mahmood, Effects of synthesis route on the structural and magnetic properties of $Sr_{1-x}RE_xFe_{12}O_{19}$ nanocrystalline hexaferrites, *Applied Physics* A, 125 (2019) 467.

16. S. Wang, J. Ding, Y. Shi, Y. Chen, High coercivity in mechanically alloyed $BaFe_{10}Al_2O_{19}$, *Journal of magnetism and magnetic materials*, 219 (2000) 206-212.

17. J.N. Dahal, L. Wang, S.R. Mishra, V.V. Nguyen, J.P. Liu, Synthesis and magnetic properties of $SrFe_{12-x-y}Al_xCo_yO_{19}$ nanocomposites prepared via autocombustion technique, *Journal of Alloys and Compounds,* 595 (2014) 213-220.

18. B.K. Rai, S.R. Mishra, V.V. Nguyen, J.P. Liu, Synthesis and characterization of high coercivity rare-earth ion doped $Sr_{0.9}RE_{0.1}Fe_{10}Al_2O_{19}$ (RE: Y, La, Ce, Pr, Nd, Sm, and Gd), *Journal of Alloys and Compounds*, 550 (2013) 198-203.

19. S. Katlakunta, S.S. Meena, S. Srinath, M. Bououdina, R. Sandhya, K. Praveena, Improved magnetic properties of Cr^{3+} doped $SrFe_{12}O_{19}$ synthesized via microwave hydrothermal route, *Materials Research Bulletin*, 63 (2015) 58-66.

20. G.A. Al-Garalleh, S.H. Mahmood, I. Bsoul, R. Loloee, Structural and magnetic properties of RE-Al substituted nanocrystalline hexaferrites $(Sr_{1-x}RE_xAl_2Fe_{10}O_{19})$, *Materials Research Express*, 7 (2020) 026103.

21. J. Lee, E.J. Lee, T.-Y. Hwang, J. Kim, Y.-H. Choa, Anisotropic characteristics and improved magnetic performance of Ca–La–Co-substituted strontium hexaferrite nanomagnets, *Scientific Reports,* 10 (2020) 15929.

22. A.H. El-Sayed, O.M. O. M. Hemeda, A. A. Tawfik, M.A. Hamad, Remarkable magnetic enhancement of type-M hexaferrite of barium in polystyrene polymer, AIP Advances, 5 (2015) 107131.

23. T. Kaur, S. Kumar, B.H. Bhat, A.K. Srivastava, Enhancement in physical properties of barium hexaferrite with substitution, *Journal of Materials Research,* 30 (2015) 2753-2762.

24. P. Güler, B. Ertuğ, N.İ. Işıkcı, A. Kara, Effect of rare-earth co-doping on the microstructural and magnetic properties of $BaFe_{12}O_{19}$, *Advances in Materials Science,* 20 (2020) 23-35.

25. S.R. Janasi, D. Rodrigues, F.J. Landgraf, M. Emura, Magnetic properties of coprecipitated barium ferrite powders as a function of synthesis conditions, Magnetics, IEEE Transactions on, 36 (2000) 3327-3329.

26. J.-P. Wang, L. Ying, M.-L. Zhang, Y.-j. QIAO, X. Tian, Comparison of the Sol-gel Method with the Coprecipitation Technique for Preparation of Hexagonal Barium Ferrite, *Chemical Research in Chinese Universities*, 24 (2008) 525-528.

27. D. Lisjak, M. Drofenik, The mechanism of the low-temperature formation of barium hexaferrite, *Journal of the European Ceramic Society,* 27 (2007) 4515-4520.

28. S. Nilpairach, W. Udomkichdaecha, I. Tang, Coercivity of the co-precipitated prepared hexaferrites, $BaFe_{12-2x}Co_xSn_xO_{19}$, *Journal of the Korean Physical Society,* 48 (2006) 939-945.

29. P. Garcia-Casillas, A. Beesley, D. Bueno, J. Matutes-Aquino, C. Martinez, Remanence properties of barium hexaferrite, *Journal of alloys and compounds*, 369 (2004) 185-189.

30. J. Matutes-Aquino, S. Dıaz-Castanón, M. Mirabal-Garcıa, S. Palomares-Sánchez, Synthesis by coprecipitation and study of barium hexaferrite powders, *Scripta materialia*, 42 (2000) 295-299.

31. P. Shepherd, K.K. Mallick, R.J. Green, Magnetic and structural properties of M-type barium hexaferrite prepared by co-precipitation, *Journal of magnetism and magnetic materials,* 311 (2007) 683-692.

32. J. Smit, H.P.J. Wijn, Ferrites, Wiley, New York, 1959.

33. M. Awawdeh, I. Bsoul, S.H. Mahmood, Magnetic properties and Mössbauer spectroscopy on Ga, Al, and Cr substituted hexaferrites, *Journal of Alloys and Compounds*, 585 (2014) 465-473.

34. B.D. Cullity, C.D. Graham, Introduction to magnetic materials, 2nd ed., John Wiley & Sons, Hoboken, NJ, 2011.

35. H.M. Lu, K. Meng, Morin Temperature and Ne´el Temperature of Hematite Nanocrystals, *Journal of Physical Chemistry* C, 114 (2010) 21291-21295.

36. M. Ahmadzadeh, C. Romero, J. McCloy, Magnetic analysis of commercial hematite, magnetite, and their mixtures, AIP Advances, 8 (2018) 056807.

37. A.M. Awadallah, S.H. Mahmood, Y. Maswadeh, I. Bsoul, A.N. Aloqaily, Structural and magnetic properties of Vanadium Doped M-Type Barium Hexaferrite ($BaFe1_{2-x}V_xO_{19}$), IOP Conference Series: *Materials Science and Engineering,* 92 (2015) 012006.

38. R. Grössinger, A critical examination of the law of approach to saturation. I. Fit procedure, *physica status solidi* (a), 66 (1981) 665-674.

39. R. Yensano, S. Phokha, Effect of pH on single phase $BaFe_{12}O_{19}$ nanoparticles and their

improved magnetic properties, *Journal of Materials Science: Materials in Electronics*, (2020) 1-10.

40. I. Abu-Aljarayesh, Basics of Magnetism, in: S.H. Mahmood, I. Abu-Aljarayesh (Eds.) Hexaferrite Permanent Magnetic Materials, *Materials Research Forum LLC, Millersville,* PA, 2016, pp. 1-46.

41. S.H. Mahmood, High Performance Permanent Magnets, in: S.H. Mahmood, I. Abu-Aljarayesh (Eds.) Hexaferrite Permanent Magnetic Materials, *Materials Research Forum LLC, Millersville*, PA, 2016, pp. 47-73.

42. S.H. Mahmood, I. Bsoul, Hopkinson peak and superparamagnetic effects in $BaFe12_{-x}Ga_xO_{19}$ nanoparticles, *EPJ Web of Conferences*, 29 (2012) 00039.